Dirhodium(II) Tetrakis(carboxamidates) with Chiral Ligands. Structure and Selectivity in Catalytic Metal-Carbene Transformations

Michael P. Doyle,*,† William R. Winchester,† Johannes A. A. Hoorn,† Vincent Lynch,*,‡ Stanley H. Simonsen,*,‡ and Ratna Ghosh‡

Contribution from the Department of Chemistry, Trinity University, San Antonio, Texas 78212, and the Department of Chemistry and Biochemistry, The University of Texas, Austin, Texas 78712

*Received March 8, 1993**

Abstract: Structure-selectivity comparisons are made between chiral dirhodium(II) tetrakis(methyl 2-oxopyrrolidine-5-carboxylates), $Rh_2(5S\text{-MEPY})_4$ and $Rh_2(5R\text{-MEPY})_4$ (**5**), and dirhodium(II) tetrakis(4-benzyl-2-oxazolidinones), $Rh_2(4R\text{-BNOX})_4$ and $Rh_2(4S\text{-BNOX})_4$ (**6**), to ascertain and understand their relative effectiveness as catalysts for enantiocontrol in metal-carbene transformations. The syntheses, spectral characteristics, and X-ray structures for these dirhodium(II) compounds are reported. Each possesses two oxygen- and two nitrogen-donor atoms bound to each octahedral rhodium with a cis orientation of the nitrogen ligands. The $Rh_2(MEPY)_4$ catalysts are significantly more effective than those of $Rh_2(BNOX)_4$ in providing a high level of enantiocontrol in intermolecular and intramolecular cyclopropanation reactions, in intermolecular cyclopropenation reactions, and in intramolecular C-H insertion reactions of diazoacetates and diazoacetamides, often reaching >90% enantiomeric excesses. Molecular mechanics calculations that were able to reproduce the X-ray structures of $Rh_2(5S\text{-MEPY})_4$ and $Rh_2(4R\text{-BNOX})_4$ have been employed to obtain the preferred conformation of the intermediate metal-carbene, but the absolute configurations of cyclopropanation products are opposite to those predicted from the preferred metal-carbene conformation. However, conformational energy minima of the styrene-carbene complex predict the observed enantiomer preference.

Dirhodium(II) compounds possessing four chiral pyrrolidone or oxazolidinone ligands are effective catalysts for highly enantioselective metal-carbene transformations.[1-4] Optical yields of greater than 90% have been achieved in olefin cyclopropanation with diazoacetate esters,[2] alkyne cyclopropenation,[3] and even carbon-hydrogen insertion reactions.[4] The basis for this high level of enantiocontrol has been attributed to the organization of the four chiral amide ligands around the dirhodium nucleus and the electronic orientation and the stabilization of the intermediate metal-carbene.[5]

A limited number of dirhodium(II) tetrakis(carboxamidate) compounds have been synthesized and characterized. Those formed from acetamide[6] and trifluoroacetamide[7] are constructed so that in the major isomer two oxygen- and two nitrogen-donor atoms (2,2) are bonded to each octadehedral rhodium in a cis configuration (eq 1). When prepared in an acetamide melt by

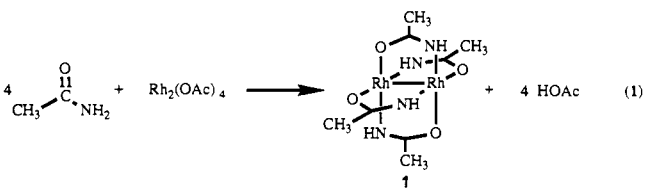

(1)

1

successive substitutions of acetate from dirhodium(II) tetraacetate, only one tetrakis(acetamidate) **1** has been obtained,[6] but with trifluoroacetamide[7] and, especially, *N*-phenylacetamide,[8] at least two of the four possible tetrasubstituted geometrical isomers are formed. The general applicability of ligand substitution methods to the synthesis of chiral dirhodium(II) carboxamides having the (2,2-cis) geometry, including a novel procedure that we recently reported for dirhodium(II) tetrakis(acetamidate), $Rh_2(acam)_4$,[9] is not evident in these investigations.

The design of dirhodium(II) catalysts that possess chiral oxazolidinone or pyrrolidone ligands in a (2,2-cis) geometry differs markedly from chiral salicylaldimine-,[10] semicorrin-,[11] and bis(oxazoline)-derived[11b,12,13] copper(I) catalysts that have been successfully employed for asymmetric intermolecular cyclopropanation reactions. The openness of these dirhodium(II) catalysts poses numerous questions regarding their viability for high enantiocontrol in metal-carbene transformations. To address these issues, we report here the syntheses, characterization, and X-ray structures of two representative dirhodium(II) compounds with chiral oxazolidinone or pyrrolidone ligands. Equilibrium constants for their coordination with acetonitrile provide an assessment of their reactivity toward diazo compounds. Comparisons of enantiocontrol and diastereocontrol in metal-carbene

† Department of Chemistry, Trinity University.
‡ Department of Chemistry and Biochemistry, University of Texas at Austin.
* Abstract published in *Advance ACS Abstracts*, October 1, 1993.

(1) Doyle, M. P.; Brandes, B. D.; Kazala, A. P.; Pieters, R. J.; Jarstfer, M. B.; Watkins, L. M.; Eagle, C. T. *Tetrahedron Lett.* **1990**, *31*, 6613.
(2) Doyle, M. P.; Pieters, R. J.; Martin, S. F.; Austin, R. E.; Oalmann, C. J.; Müller, P. *J. Am. Chem. Soc.* **1991**, *113*, 1423.
(3) Doyle, M. P.; van Oeveren, A.; Westrum, L. J.; Protopopova, M. N.; Clayton, T. W., Jr. *J. Am. Chem. Soc.* **1991**, *113*, 8982.
(4) Protopopova, M. N.; Doyle, M. P.; Müller, P.; Ene, D. *J. Am. Chem. Soc.* **1992**, *114*, 2755.
(5) Doyle, M. P. *Recl. Trav. Chim. Pays-Bas* **1991**, *110*, 305.
(6) Ahsan, M. Q.; Bernal, I.; Bear, J. L. *Inorg. Chem.* **1986**, *25*, 260.
(7) Dennis, A. M.; Korp, J. D.; Bernal, I.; Howard, R. A.; Bear, J. L. *Inorg. Chem.* **1983**, *22*, 1522.
(8) Lifsey, R. S.; Lin, X. Q.; Chavan, M. Y.; Ahsan, M. Q.; Kadish, K. M.; Bear, J. L. *Inorg. Chem.* **1987**, *26*, 830.
(9) Doyle, M. P.; Bagheri, V.; Wandless, T. J.; Harn, N. K.; Brinker, D. A.; Eagle, C. T.; Loh, K.-L. *J. Am. Chem. Soc.* **1990**, *112*, 1906.
(10) Aratani, T. *Pure Appl. Chem.* **1985**, *57*, 1839.
(11) (a) Fritschi, H.; Leutenegger, U.; Pfaltz, A. *Angew. Chem., Int. Ed. Engl.* **1986**, *25*, 1005. (b) Müller, D.; Umbricht, G.; Weber, B.; Pfaltz, A. *Helv. Chim. Acta* **1991**, *74*, 232. (c) Fritschi, H.; Leutenegger, U.; Siegmann, K.; Pfaltz, A.; Keller, W.; Kratky, Ch. *Helv. Chim. Acta* **1988**, *71*, 1541. (d) Fritschi, H.; Leutenegger, U.; Umbricht, G.; Fahrni, C.; Vonmatt, P.; Pfaltz, A. *Tetrahedron* **1992**, *48*, 2143.
(12) (a) Lowenthal, R. E.; Abiko, A.; Masamune, S. *Tetrahedron Lett.* **1990**, *31*, 6005. (b) Lowenthal, R. E.; Masamune, S. *Tetrahedron Lett.* **1991**, *32*, 7373.
(13) (a) Evans, D. A.; Woerpel, K. A.; Himman, M. M. *J. Am. Chem. Soc.* **1991**, *113*, 726. (b) Evans, D. A.; Woerpel, K. A.; Scott, M. J. *Angew. Chem., Int. Ed. Engl.* **1992**, *31*, 430.

0002-7863/93/1515-9968$04.00/0

reactions catalyzed by representatives of these dirhodium(II) catalysts define the structural features of the dirhodium(II) ligands that control their selectivity. Finally, comparative reactivity/selectivity data and computations of relative energy differences suggest the stereoelectronic and steric factors that contribute to the effectiveness of these catalysts for highly enantioselective transformations.

Results

Synthesis and Characterization. Treatment of $Rh_2(OAc)_4$ with excess chiral oxazolidinone or pyrrolidone (L*H = **2**–**4**) in refluxing chlorobenzene causes the sequential replacement of the acetate ligand by the targeted carboxamide. Acetic acid is

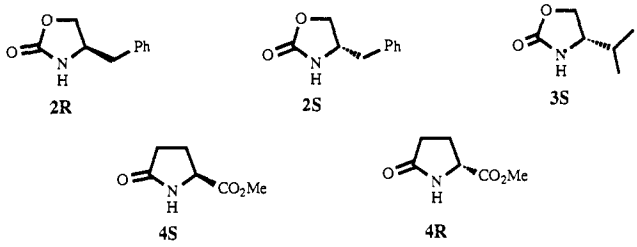

captured by sodium carbonate in a Soxhlet extractor, thereby forcing the ligand substitution reaction to completion (eq 2).

$$Rh_2(OAc)_4 + 4L^*H \rightarrow Rh_2L^*_4 + 4HOAc \qquad (2)$$

These reactions may be followed by HPLC analyses, and although minor amounts of reaction byproducts are formed, only one tetrasubstituted $Rh_2L^*_4$[Rh_2(4*S*-BNOX)$_4$, Rh_2(4*R*-BNOX)$_4$, Rh_2(4*S*-IPOX)$_4$, Rh_2(5*S*-MEPY)$_4$, or Rh_2(5*R*-MEPY)$_4$, where BNOX = 4-benzyl-2-oxazolidinone, IPOX = 4-isopropyl-2-oxazolidinone, and MEPY = methyl 2-oxopyrrolidine-5-carboxylate] is produced. Displacement reactions with oxazolidinones generally occur over a longer time (24 h) than those with pyrrolidones (6 h). Removal of acetic acid is essential to the success of this ligand substitution method, and as might be expected, increasing the concentration of the reactants increases the rate of substitution. In all cases, the third and fourth ligands are added at much slower rates than the first two.

The NMR spectra of these dirhodium(II) compounds are consistent with the (2,2-cis) ligand geometry. The ^{1}H NMR spectrum of dirhodium(II) tetrakis[methyl 2-oxopyrrolidine-5(*R*)-carboxylate], Rh_2(5*R*-MEPY)$_4$, for example, exhibits absorptions at δ 4.32 and 3.95 corresponding to hydrogens at C5 that are bonded to the asymmetric center in the two nonequivalent sets of ligands. Furthermore, two resonances are observed for each carbon of methyl 2-oxopyrrolidine-5(*R*)-carboxylate in Rh_2(5*R*-MEPY)$_4$. These spectral data correspond to the (2,2-cis) geometry for Rh_2(5*R*-MEPY)$_4$ which would be predicted to possess two sets of magnetically nonequivalent protons or carbons for each position in the ligated methyl 2-oxopyrrolidine-5(*R*)-carboxylate. The dirhodium(II) compound having the (2,2-trans) geometry, with its C_2 axis through the Rh–Rh bond, would have exhibited a single resonance or set of resonances for each ^{1}H or ^{13}C of the bound methyl 2-oxopyrrolidine-5(*R*)-carboxylate, and by similar arguments, the (3,1) and (4,0) isomers can also be excluded. Similar structural assignments can be made from the NMR spectra of each of the tetrasubstituted dirhodium(II) compounds possessing ligands **2**–**4**.

Structural Studies: Rh_2(5*R*-MEPY)$_4$ and Rh_2(4*S*-BNOX)$_4$. The structure of the bis(acetonitrile) complex of dirhodium(II) tetrakis[methyl 2-oxopyrrolidine-5(*R*)-carboxylate], Rh_2(5*R*-MEPY)$_4$(CH$_3$CN)$_2$(*i*-PrOH), was determined by X-ray diffraction analysis of a crystal grown from acetonitrile/2-propanol (**5**, Figure 1). The (2,2-cis) geometry, which had been deduced from NMR data and previously observed in dirhodium(II) complexes

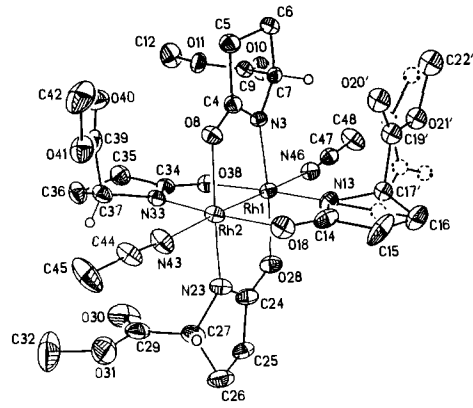

Figure 1. Thermal ellipsoid representation of Rh_2(5*R*-MEPY)$_4$(CH$_3$CN)$_2$(*i*-PrOH) (**5**) showing the atom-labeling scheme. The nonhydrogen atoms are scaled to the 30% probability level. Most hydrogen atoms are omitted for clarity. The atoms of the minor (45(1)%) component of the disordered carboxylate group are illustrated as dashed circles.

with bridging achiral amide ligands, was confirmed. Viewed along the Rh–Rh axis, the nearest carboxylate groups are positioned with a clockwise orientation, while those at the far end have a counterclockwise orientation, consistent with the (*R*)-configuration. Four quadrants defined by the O–Rh and N–Rh bonds down through the Rh–Rh bond axis are evident in this structure. This crystalline form contains one molecule of 2-propanol that is disordered about two positions. In each position, the alcohol oxygen is within H-bonding distance of a coordinated carbonyl oxygen, O23 2.90(2) Å and O18 2.75(2) Å. In the crystal lattice, the solvent lies in channels formed by the open quadrant of the Rh–Rh complex.

The ester carbonyl oxygen O10 is situated only 3.15 Å from the carbon atom of the nearby acetonitrile. The other three carbonyl oxygens are located at greater distances from the carbon atom of the axially bound acetonitrile. One of the acetonitrile molecules is bound to rhodium with a Rh–N bond length of 2.215 Å, while the other has a Rh–N bond length of 2.236 Å. The Rh–Rh bond distance for Rh_2(5*R*-MEPY)$_4$(CH$_3$CN)$_2$(*i*-PrOH) is longer than those for Rh_2(OAc)$_4$(H$_2$O)$_2$ (2.386 Å),[14] Rh_2(OAc)$_4$(CH$_3$CN)$_2$ (2.384 Å),[15] Rh_2(acam)$_4$(H$_2$O)$_2$ (2.415 Å),[6] and Rh_2(vall)$_4$(Hvall)$_2$ (2.392 Å, Hvall = δ-valerolactone)[16] but nearly the same as that for Rh_2(pyro)$_4$(Hpyro)$_2$ (2.445 Å, Hpyro = 2-pyrrolidone).[16] The average O–Rh distance of 2.079 Å in Rh_2(5*R*-MEPY)$_4$(CH$_3$CN)$_2$ is longer than the average N–Rh distance of 2.015 Å, imparting a slight tilt to the ligand that moves the methyl carboxylate closer to the axial coordination site of rhodium. A summary of the crystallographic and data collection parameters is given in Table I. Selected interatomic distances and angles for Rh_2(5*R*-MEPY)$_4$(CH$_3$CN)$_2$(*i*-PrOH) are presented in Table II.

The structure of the bis(acetonitrile) complex of dirhodium(II) tetrakis[4(*S*)-benzyl-2-oxazolidinone], Rh_2(4*S*-BNOX)$_4$(CH$_3$CN)$_2$(CH$_3$CN), was determined by X-ray diffraction analysis of a crystal grown from acetonitrile (**6**, Figure 2). In addition to the two axially ligated acetonitriles, one additional acetonitrile molecule appears in the crystalline lattice. Like the Rh_2(5*R*-MEPY)$_4$ structure described in Figure 1, the oxazolidinone ligands adopt a (2,2-cis) geometry with the nearest benzyl groups oriented clockwise and the distant benzyl groups oriented counterclockwise when viewed along the Rh–Rh bond axis. The phenyl substituents are rotated away from the axial acetonitrile ligands of dirhodium(II), creating a more open atomic arrangement in this structure.

(14) Cotton, F. A.; DeBoer, B. G.; LaPrade, M. D.; Pipal, J. R.; Veko, D. A. *J. Am. Chem. Soc.* **1970**, *92*, 2926.
(15) Cotton, F. A.; Thompson, J. L. *Acta Crystallogr. Sect. B* **1981**, *37*, 2235.
(16) Bear, J. L.; Lifsey, R. S.; Chau, L. K.; Ahsan, M. Q.; Korp, J. D.; Chavan, M.; Kadish, K. M. *J. Chem. Soc., Dalton Trans.* **1989**, 93.

Table I. Crystallographic Data for $Rh_2(5R\text{-MEPY})_4(CH_3CN)_2(i\text{-PrOH})$ (**5**) and $Rh_2(4S\text{-BNOX})_4(CH_3CN)_2(CH_3CN)$ (**6**)[a]

	5	**6**
formula	$C_{31}H_{46}N_6O_{13}Rh_2$	$C_{46}H_{49}N_7O_8Rh_2$
fw	916.55	1033.75
a, Å	10.058(4)	10.425(6)
b, Å	19.018(8)	17.871(8)
c, Å	19.609(5)	24.188(6)
V, Å^3	3751(2)	4506(3)
Z	4	4
crystal system	orthorhombic	orthorhombic
space group	$P2_12_12_1$ (No. 19)	$P2_12_12_1$ (No. 19)
T, °C	−80	−80
radiation	graphite monochromatized, Mo	Kα (λ = 0.7107 Å)
2θ range (degrees)	4–55	4–55
scan speed (degrees/min) (1.2° ω scan)	4–8	3–6
ρ_{calc}, g/cc	1.62	1.52
reflections measured	8631	5431
unique reflections	4874	5431
R_{int}	0.031	not applicable
μ, cm^{-1}	9.322	7.785
transmission factor[b] range	0.6416–0.8043	0.6486–0.8185
crystal size, mm	0.3 × 0.5 × 0.5	0.1 × 0.2 × 0.3
reflections used	4427	3736
reflections rejected	447 [$F < 4(\sigma(F))$]	1695 [$F < 6(\sigma F)$)]
secondary extinction[c] correction factor	$3.8(6) \times 10^{-7}$	insignificant, not applied
$R(F)$[d]	0.0431	0.0383
$R_w(F)$	0.0467	0.0487
goodness of fit	1.46	1.351
parameters	449	568
max $\lvert\Delta/\sigma\rvert$	<0.1	<0.1
min, max peaks (e/Å^3)	−0.49, 0.93	−0.78, 1.54
M parameter	1.2(1)	1.0(1)

[a] Data for both samples were collected on a Nicolet P3 diffractometer using a Nicolet LT-2 low-temperature delivery system. Lattice parameters were obtained from the least-squares refinement of 30 reflections with 18.6° < 2θ < 23.7° for **6** and 31 reflections with 19.0° < 2θ < 21.8° for **5**. [b] Absorption correction was based on measured crystal faces. [c] The correction for secondary extinction is of the form: $F_{corr} = F_{calc}/[(1 + X)(F_{calc})^2/\sin^2\theta]^{1/4}$ where X is the correction factor. [d] The function $\sum w(|F_o| - |F_c|)^2$ was minimized and where $w = 1/(\sigma(F_o)^2 + (0.02F)^2)$.

Table II. Selected Interatomic Distances (Å) and Angles (degrees) for $Rh_2(5R\text{-MEPY})_4(CH_3CN)_2(i\text{-PrOH})$ (**5**)[a]

Distances							
Rh1–Rh2	2.4570(10)	C4–N3	1.302(7)	O8–Rh2	2.088(4)	C9–C7	1.524(8)
N3–Rh1	2.018(4)	C7–N3	1.448(6)	O18–Rh2	2.074(4)	O10–C9	1.183(7)
N13–Rh1	2.012(5)	C5–C4	1.492(8)	N23–Rh2	2.009(5)	O11–C9	1.335(7)
O28–Rh1	2.081(4)	O8–C4	1.267(6)	N33–Rh2	2.022(5)	O11–C12	1.424(8)
O38–Rh1	2.071(4)	C6–C5	1.550(8)	N43–Rh2	2.236(4)		
N46–Rh1	2.215(4)	C7–C6	1.544(7)				
Angles							
Rh2–Rh1–N3	84.76(11)	C4–N3–Rh1	123.3(3)	N3–Rh1–O38	89.3(2)	C7–C6–C5	102.7(4)
Rh2–Rh1–N13	85.73(13)	C7–N3–Rh1	124.7(3)	N3–Rh1–N46	95.1(2)	C9–C7–N3	112.9(4)
Rh2–Rh1–O28	90.59(11)	O8–C4–N3	126.6(5)	N46–Rh1–Rh2	178.80(14)	O10–C9–C7	124.8(5)
Rh2–Rh1–O38	98.94(10)	C6–C5–C4	102.8(5)	N43–Rh2–Rh1	177.6(2)	O10–C9–O11	124.7(5)
N3–Rh1–N13	91.8(2)	C5–C4–O8	120.7(5)	C4–N3–C7	111.8(4)	C12–O11–C9	114.7(5)
N3–Rh1–O28	175.0(2)	C5–C4–N3	112.6(5)				

[a] Estimated standard deviations in the least significant digit are given in parentheses.

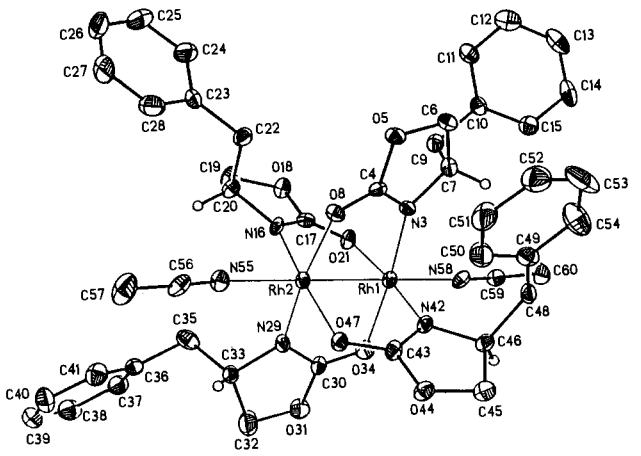

Figure 2. Thermal ellipsoid representation of $Rh_2(4S\text{-BNOX})_4(CH_3CN)_2(CH_3CN)$ (**6**) showing the atom-labeling scheme. The non-hydrogen atoms are scaled to the 30% probability level. Most hydrogen atoms are omitted for clarity.

The carbamate functionality of the ligated oxazolidinone might have been expected to increase the electron density at rhodium, thereby influencing the bond lengths to rhodium. The average O–Rh bond length of 2.088 Å and average N–Rh bond length of 2.019 Å of **6** are slightly longer than those of **5**, but the average N–Rh bond distance of 2.226 Å for the axial acetonitrile ligands is not different. The Rh–Rh bond length in **6** of 2.472(2) Å is 0.01 Å longer than that in **5**. Interestingly, **5**, **6**, and $Rh_2(pyro)_4(Hpyro)_2$[16] all have much longer Rh–Rh bond lengths than do $Rh_2(acam)_4(H_2O)_2$[6] or $Rh_2(vall)_4(Hvall)_2$,[16] up to 0.08 Å. Since this difference is unlikely to be due to electronic factors, its cause may be attributed to the opening of the carbonyl oxygen–amide nitrogen distance (the NCO bite) by the five-membered ring. A summary of the crystallographic and data collection parameters is given in Table I. Selected interatomic distances and angles for $Rh_2(4S\text{-BNOX})_4(CH_3CN)_2(CH_3CN)$ are presented in Table III.

Association with Acetonitrile. Equilibrium constants for the association of acetonitrile with $Rh_2(5R\text{-MEPY})_4$ and $Rh_2(4S\text{-BNOX})_4$ were measured in 1,2-dichloroethane by successive addition of the nitrile to the dirhodium(II) compounds possessing

Table III. Selected Interatomic Distances (Å) and Angles (degrees) for $Rh_2(5S\text{-BNOX})_4(CH_3CN)_2(CH_3CN)$ (6)[a]

			Distances				
Rh1–Rh2	2.472(2)	C4–N3	1.309(13)	N16–Rh2	2.046(7)	C9–C7	1.554(13)
N3–Rh1	2.011(7)	C7–N3	1.465(12)	N29–Rh2	2.007(8)	C10–C9	1.525(13)
N42–Rh1	2.011(7)	O5–C4	1.361(10)	O47–Rh2	2.087(5)	C10–C11	1.356(13)
O21–Rh1	2.090(6)	O8–C4	1.267(11)	O8–Rh2	2.091(6)	C15–C10	1.386(14)
O34–Rh1	2.085(7)	C6–O5	1.444(11)	N55–Rh2	2.252(8)		
N58–Rh1	2.205(8)	C7–C6	1.531(14)				
			Angles				
Rh1–Rh2–N16	84.3(2)	C4–N3–Rh1	121.9(6)	N3–Rh1–O21	91.3(3)	C7–C6–O5	104.9(7)
Rh1–Rh2–N29	84.8(2)	C7–N3–Rh1	129.8(6)	N3–Rh1–N58	95.8(3)	C9–C7–N3	111.3(7)
Rh1–Rh2–O47	89.7(2)	O8–C4–N3	127.6(8)	N58–Rh1–Rh2	179.1(2)	C10–C9–C7	112.6(7)
Rh1–Rh2–O8	89.4(2)	C6–O5–C4	106.6(7)	N55–Rh2–Rh1	178.7(2)	C15–C10–C9	120.0(9)
N3–Rh1–N42	90.5(3)	O5–C4–O8	116.9(9)	C4–N3–C7	108.2(7)	C11–C10–C9	121.5(9)
N3–Rh1–O34	174.6(3)	O5–C4–N3	115.5(8)				

[a] Estimated standard deviations in the least significant digit are given in parentheses.

Table IV. Spectrophotometric Analysis of the Equilibrium Association of Dirhodium(II) Compounds with Acetonitrile at 25 °C

			λ_{max}, nm		
$Rh_2l^*_4$	K_1, M^{-1}	K_2, M^{-1}	$Rh_2L^*_4$	$Rh_2L^*_4 \cdot CH_3CN$	$Rh_2L_4 \cdot 2CH_3CN$
$Rh_2(5R\text{-MEPY})_4$[a]	65 ± 6	2.2 ± 0.2	615	560	505
$Rh_2(4S\text{-BNOX})_4$[b]	102 ± 9	1.4 ± 0.2	590	565	510

[a] Isosbestic points were observed at 595 and 520 nm. [b] Isosbestic points were observed at 580 and 525 nm.

open axial coordination sites (Table IV). An isosbestic point was associated with each equilibrium defined by eqs 3 and 4. As with earlier studies of equilibrium association of dirhodium(II) carboxylates with acetonitrile,[17] the first equilibrium constant K_1

$$Rh_2L^*_4 + CH_3CN \overset{K_1}{\rightleftharpoons} Rh_2L^*_4(CH_3CN) \quad (3)$$

$$Rh_2L^*_4(CH_3CN) + CH_3CN \overset{K_2}{\rightleftharpoons} Rh_2L^*_4(CH_3CN)_2 \quad (4)$$

for association of the dirhodium(II) compound with CH_3CN, was found to be larger than the second equilibrium constant K_2. However, these values are more than an order of magnitude lower than those for dirhodium(II) butyrate ($K_1 = 1.7 \times 10^3$, $K_2 = 27.0$)[17a] and more than 3 orders of magnitude lower than those for dirhodium(II) perfluorobutyrate ($K_1 = 1.43 \times 10^5$, $K_2 = 4.53 \times 10^3$).[17b] These equilibrium constants, especially K_1, gauge the reactivity of dirhodium(II) compounds toward diazo compounds. Whereas dirhodium(II) carboxylates effectively and efficiently

Table V. Comparisons of Enantioselectivities (diastereoselectivities) in Metal–Carbene Transformations Catalyzed by $Rh_2(4R\text{-BNOX})_4$ and $Rh_2(5S\text{-MEPY})_4$

catalytic transformation	eq no.		% ee (de)[a] $Rh_2(4R\text{-BNOX})_4$	% ee (de)[a] $Rh_2(5S\text{-MEPY})_4$
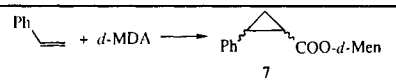 7	(5)	cis trans	62 (1*S*,2*R*)[b] 34 (1*S*,2*S*)[b]	86 (1*S*,2*R*)[c] 48 (1*S*,2*S*)[c]
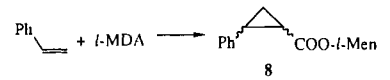 8	(6)	cis trans	25 (1*S*,2*R*)[b] 4 (1*S*,2*S*)[b]	79 (1*S*,2*R*)[c] 56 (1*S*,2*S*)[c]
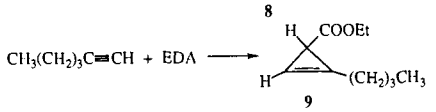 9	(7)		5	57[d]
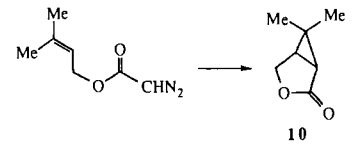 10	(8)		56 (1*S*,5*R*)	98 (1*S*,5*R*)[e]
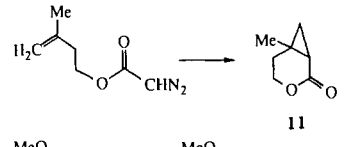 11	(9)		28 (1*S*,6*R*)	79 (1*S*,6*R*)[f]
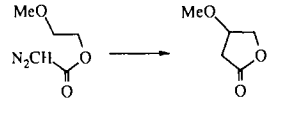 12	(10)		11 (*S*)	91 (*S*)[g]
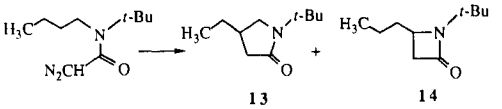 13 14	(11)	13 14	<2 (92%) 0 (8%)	63 (88%)[h] 73 (12%)[h]

[a] Where known, absolute configurations are given in parentheses. Abbreviations: *d*-MDA = (+)-(1*S*,2*R*,5*S*)-2-isopropyl-5-methyl-1-cyclohexyl diazoacetate; *d*-Men = (+)-(1*S*,2*R*,5*S*)-2-isopropyl-5-methyl-1-cyclohexyl; EDA = ethyl diazoacetate. [b] Reference 1, trans:cis = 67:33 for *d*-MDA and 62:38 for *l*-MDA. [c] Reference 20, trans:cis = 57:43 for *d*-MDA and 52:48 for *l*-MDA. [d] Reference 2, % ee is 6% higher than that previously reported; value based on GC analyses with a Chiraldex γ-TFA column. [f] Reference 21. [g] Reference 3. [h] Reference 22, relative yields in parentheses.

catalyze the decomposition of α-diazo β-keto esters at 80 °C, and with dirhodium(II) perfluorobutyrate these reactions occur at 40 °C,[18] the dirhodium(II) catalysts possessing ligands **2–4** are ineffective at 80 °C over several hours with the same substrates. Absorption maxima for the two dirhodium(II) compounds that are reported in Table IV are similar to that of $Rh_2(acam)_4(CH_3CN)_2$ (λ_{max} = 500 nm).[19] The oxazolidinone derivative $Rh_2(4S\text{-BNOX})_4$ has the higher value for K_1, and indeed, this compound is a more reactive catalyst toward diazo compounds (rate of nitrogen evolution).

Asymmetric Catalysis. Applications of $Rh_2(MEPY)_4$ and $Rh_2(BNOX)_4$ in either or both enantiomeric structures to intermolecular and intramolecular cyclopropanation, intermolecular cyclopropenation, and carbon–hydrogen insertion reactions of diazoacetates or diazoacetamides reveal striking differences in enantioselection. Results from the uses of $Rh_2(4R\text{-BNOX})_4$ and $Rh_2(5S\text{-MEPY})_4$ show that $Rh_2(5S\text{-MEPY})_4$ is significantly more effective than $Rh_2(4R\text{-BNOX})_4$ (Table V), and the degree of difference in enantioselectivity (diastereoselectivity) that is observed varies with the transformation. For intermolecular cyclopropanation of styrene, the use of *d*- or *l*-menthyl diazoacetate (*d*- or *l*-MDA) does not greatly influence product diastereoselectivity with $Rh_2(5S\text{-MEPY})_4$[20] but substantial differences in % de result from the use of $Rh_2(4R\text{-BNOX})_4$.[1] Enantioselectivity is reduced in nearly proportional fashion for intramolecular cyclopropanation by the use of $Rh_2(4R\text{-BNOX})_4$ from that achieved with $Rh_2(5S\text{-MEPY})_4$ (eqs 8 and 9).[2,21] However, in intermolecular cyclopropenation and C–H insertion reactions, $Rh_2(4R\text{-BNOX})_4$ is ineffective in providing even a modest level of stereocontrol (eqs 7, 10, and 11).[3,22] Results similar to those obtained with $Rh_2(BNOX)_4$ catalysts have been obtained in selected cases with dirhodium(II) tetrakis[4(*S*)-isopropyl-2-oxazolidinone], $Rh_2(4S\text{-IPOX})_4$: eq 5, 4% de (1*R*,2*S*)-cis-**7**, 2% de (1*R*,2*R*)-trans-**7**; eq 6, 56% de (1*R*,2*S*)-cis-**8**, 34% de (1*R*,2*R*)-trans-**8**; and eq 8, 43% ee (1*R*,5*S*)-**10**.

Further differences between $Rh_2(BNOX)_4$ and $Rh_2(MEPY)_4$ catalysts occur in reactivity/selectivity for intramolecular cyclopropanation of 3-methyl-2-buten-1-yl diazoacetate, where butenolide **15** is observed in addition to the bicyclic lactone **16** (eq 12). Although the relative yield of **15** is low, its presence

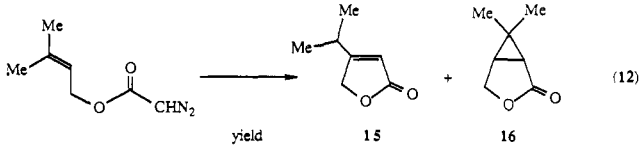

(12)

	yield	15	16
$Rh_2(4R\text{-BNOX})_4$	62%	19	81 (56% ee)
$Rh_2(4S\text{-BNOX})_4$	63%	17	83 (55% ee)
$Rh_2(5S\text{-MEPY})_4$	82%	<1	>99 (98% ee)
$Rh_2(5R\text{-MEPY})_4$	83%	<1	>99 (98% ee)

signifies a mechanistic pathway which has long been known in electrophilic metal–carbene additions to alkenes that are able to form relatively stable carbocations. In these cases, concerted cycloaddition can occur in competition with stepwise electrophilic addition of the metal–carbene to form a 3° carbocation intermediate followed by 1,2-hydride transfer that is concurrent with dissociation of the dirhodium(II) catalyst (Scheme I), and it is

Scheme I

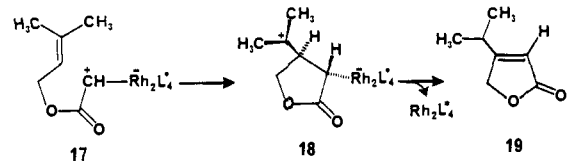

from this stepwise addition pathway that butenolide **15** can be assumed to arise. The relative yield of **15** from reactions catalyzed by $Rh_2(4S\text{-IPOX})_4$ is 10% (49% yield **14** + **15**, 43% ee **16**). A similar process has recently been uncovered in an intramolecular cyclopropanation of a diazo ketone, and its relative importance was related to the electrophilicity of the dirhodium(II) catalyst.[23] Also, Alonso has reported cationic rearrangement byproducts from intermolecular cyclopropanation reactions that are consistent with Scheme I,[24] and the well-known "apparent" allylic C–H insertion transformation from reactions of diazomalonates with alkenes,[25] originally reported by Wenkert,[26] also follows this reaction pathway.

The integrity of these dirhodium(II) catalysts is maintained during the metal–carbene reactions. In those instances where the catalyst was recovered for analysis, greater than 90% of the intact dirhodium(II) compound, as determined by spectral and HPLC analyses, was obtained. Furthermore, in the vast majority of cases, the initial blue-green solution color of the catalyst returns in the catalyst isolated after addition of the yellow diazo compound has terminated.

Computational Modeling. The structures of these dirhodium(II) catalysts and their presumed carbene intermediates have been investigated with molecular mechanics and molecular orbital methods. Our approach is to use molecular mechanics calculations to model steric effects and extended Hückel calculations to examine electronic effects. These studies are simplified by the limited rotational degrees of freedom from the bridging cyclic carboxamides such as are found in $Rh_2(5R\text{-MEPY})_4$ and $Rh_2(4S\text{-BNOX})_4$ which reduces the complexity of searching the potential energy surface. The molecular mechanics program employs Allinger's MM2 force field[27] which has been extended to the full periodic table.

The nature of the Rh–Rh bond in dirhodium(II) carboxylates has been the subject of numerous computational studies, from molecular mechanics to *ab initio* molecular orbital methods.[28–33] These studies have concluded that the dirhodium(II) carboxylates possess a Rh–Rh single bond and that the effect of axial ligands can be quite complex, often changing the relative ordering of the orbitals resulting from metal–metal bonding. These results will prove useful in further discussions of bonding in carbene complexes, but our initial interest is in the correct prediction of

(17) (a) Drago, R. S.; Long, J. R.; Cosmano, R. *Inorg. Chem.* **1981**, *20*, 2920. (b) Drago, R. S.; Long, J. R.; Cosmano, R. *Inorg. Chem.* **1982**, *21*, 2196.

(18) (a) Doyle, M. P.; Shanklin, M. S.; Pho, H. Q.; Mahapatro, S. N. *J. Org. Chem.* **1988**, *53*, 1017. (b) Doyle, M. P.; Westrum, L. J.; Wolthuis, W. N. E.; See, M. M.; Boone, W. P.; Bagheri, V.; Pearson, M. M. *J. Am. Chem. Soc.* **1993**, *115*, 958.

(19) Chavan, M. Y.; Zhu, T. P.; Lin, X. Q.; Ahsan, M. Q.; Bear, J. L.; Kadish, K. M. *Inorg. Chem.* **1984**, *23*, 4538.

(20) Doyle, M. P.; Protopopova, M. N.; Brandes, B. D.; Davies, H. M. L.; Huby, N. J. S.; Whitesell, J. K. *Synlett* **1993**, 151.

(21) Martin, S. F.; Oalmann, C. J.; Liras, S. *Tetrahedron Lett.* **1992**, *33*, 6727.

(22) Doyle, M. P.; Protopopova, M. N.; Winchester, W. R.; Daniel, K. L. *Tetrahedron Lett.* **1992**, *33*, 7819.

(23) Padwa, A.; Austin, D. J.; Price, A. T.; Semones, M. A.; Doyle, M. P.; Protopopova, M. N.; Winchester, W. R.; Tran, A. *J. Am. Chem. Soc.* **1993**, *115*, 8669.

(24) (a) Alonso, M. E.; Fernandez, R. *Tetrahedron* **1989**, *45*, 3313. (b) Alonso, M. E.; del Carmon Garcia, M. *J. Org. Chem.* **1985**, *50*, 988.

(25) (a) Doyle, M. P. *Chem. Rev.* **1986**, *86*, 919. (b) Doyle, M. P. *Acc. Chem. Res.* **1986**, *19*, 348. (c) Mass, G. *Top. Current Chem.* **1987**, *137*, 75.

(26) Wenkert, E.; Alonso, M. E.; Buckwalter, B. L.; Sanchez, E. L. *J. Am. Chem. Soc.* **1983**, *105*, 2021.

(27) Burkert, U.; Allinger, N. L. *Molecular Mechanics*; ACS Monograph 177; American Chemical Society: Washington, DC, 1982.

(28) Bear, J. L.; Yao, C.-L.; Liu, L.-M.; Capdevielle, F. J.; Korp, J. D.; Albright, T. A.; Kang, S.-K.; Kadish, K. M. *Inorg. Chem.* **1989**, *28*, 1254 and references cited therein.

(29) Cotton, F. A.; Walton, R. A. *Multiple Bonds Between Metal Atoms*; R. E. Krieger Publishing Co.: Malabar, FL, 1988; p 369.

(30) (a) Norman, J. G., Jr.; Kolari, H. J. *J. Am. Chem. Soc.* **1978**, *100*, 791. (b) Norman, J. G., Jr.; Renzoni, G. E.; Case, C. A. *J. Am. Chem. Soc.* **1979**, *101*, 5256.

(31) (a) Boeyens, J. C. A.; Cotton, F. A.; Han, S. *Inorg. Chem.* **1985**, *24*, 1750. (b) Bursten, B. E.; Cotton, F. A. *Inorg. Chem.* **1981**, *20*, 3042.

(32) (a) Nakatsuji, H.; Ushio, J.; Kanda, K.; Onishi, Y.; Kawamura, T.; Yonezawa, T. *Chem. Phys. Lett.* **1981**, *79*, 299. (b) Sowa, T.; Kawamura, T.; Shida, T.; Yonezawa, T. *Inorg. Chem.* **1983**, *22*, 56.

(33) O'Neill, F. M.; Boeyens, J. C. A. *Inorg. Chem.* **1990**, *29*, 1301.

the lowest energy conformation and the relative energies of metal–carbene conformations. These depend upon conformational changes in the ligands and should have little effect on bonding in the dirhodium core.

The suitability of the molecular mechanics parameters for these determinations was tested by placing X-ray structure determinations into the molecular mechanics program and optimizing the structure. It is unlikely that these structures are global minima, and it is not necessary that they would be the most populated conformations in solution. But they are certainly local minima, and in as much as they allow us to test our ability to find local minima, the comparisons lend confidence into the validity of this approach.

For $Rh_2(5R\text{-MEPY})_4(CH_3CN)_2$, the optimized structure showed slight changes in geometry from the X-ray structure. The average difference in bond length (excluding hydrogens and acetonitrile) between the calculated and observed structure was 0.032 Å, with most differences being less than half this value. Delocalization between the nitrogen lone pair and the carbonyl is not modeled well, so that the calculated N—C bond is too long by 0.12 Å and the C=O bond is too short by 0.06 Å. The dihedral angles, which we expected to be more challenging to calculate, are well modeled—the ring puckering (C–C–C–C) is calculated to be 21.9° (MM) and found to be 20.1° (X-ray). The carboxylate carbonyl dihedral angle is calculated to be −132.3° (MM) and found to be −124.7°.

Because of the potential for carbene stabilization by the ligand carboxylate substituents, the distance between the carbonyl oxygens of $Rh_2(5R\text{-MEPY})_4(CH_3CN)_2$ and the acetonitrile ligand is a critical parameter. The O10′–N46′ and O40′–N43′ calculated distances, 3.37 and 4.72 Å, respectively, correspond remarkably well to those from X-ray structures, 3.28 and 4.67 Å, respectively. The same is true for the O10′–C47′ and O40′–C44′ distances: 3.15 and 5.14 Å, respectively, by X-ray and 3.31 and 5.23 Å, respectively, by molecular mechanics calculations. The agreement is all the more remarkable when one considers that it reflects not a single bond distance but the distance resulting from the combination of the many bond distances, bond angles, and dihedral angles that make up the ring connecting these atoms. For O20′–N46′ and O40′–N43′, the agreement is less good, the differences being 0.2–0.3 Å between calculated and observed, and this may be due to perturbations by 2-propanol in the crystalline lattice.

For $Rh_2(4S\text{-BNOX})_4(CH_3CN)_2$, the optimized structure and the experimentally observed structure are again very similar. The average difference in bond lengths is again small (0.03 Å). The C=O distance is longer than that calculated by 0.059 Å, and the C—N distance is shorter than that calculated by 0.111 Å. Once again, the dihedral angles were accurately reproduced. The oxazolidinone ring is less puckered than the pyrrolidinone ring, and this greatly affects the positioning of the benzyl substituent at the chiral center relative to the axial coordination site at rhodium. The influence of oxygen substitution for carbon, which was expected to pull the substituent away because of the shorter carbon–oxygen bond, is negated by the lack of out-of-plane bending in the oxazolidinone ring.

Convinced of the reliability of the modeling parameters in predicting catalyst structure, we investigated the structure of the carbene intermediate, for which there is no experimentally available comparison, with a metal–carbene model—$Rh_2(acam)_4{=}CH_2$. The acetamide ligand avoids most steric effects and allows the study of the electronic barrier to carbene rotation about the (metal–carbene)–carbon bond in $Rh_2(acam)_4{=}CH_2$. Because of the known deficiency of extended Hückel calculations for optimizing structures, all structures used are those from molecular mechanics. The structures were generated by optimizing the carbene and then rotating it as a rigid rotor in 15° intervals upon which extended Hückel calculations were performed. The molecular mechanics calculated barrier to rotation was less than 1 kcal/mol with the minimum at 45°, and the barrier calculated using extended Hückel was again less than 1 kcal/mol. Thus, any conformational preference for $Rh_2(MEPY)_4$- or $Rh_2(BNOX)_4$-bound carbenes will not be due to an electronic rotational barrier in the dirhodium(II) complexes.

To model the steric and electronic effects of chiral ligands on a bound carbene, we selected the hypothetical $Rh_2(5S\text{-MEPY})_2(acam)_2$ (**20**) to which was attached carbomethoxycarbene. This

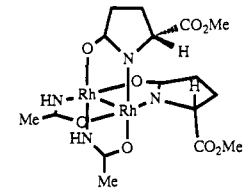

20

structure contains the minimum elements required to model steric and electronic interactions between the bound carbene and the chiral ligands of rhodium(II). To find the global minima, the carbomethoxycarbene was rotated through 360° in steps of 15° and the two ligand carboxylate groups were rotated through 360° in steps of 45° with each point being fully optimized except for the restriction of the search variables using molecular mechanics. The minima found from an analysis of the molecular mechanics search were then saved as separate files and resubmitted for optimization. Three conformational minima (**21–23**) for carbene rotations, each significantly different in energy, result from these computations (Chart I). Multiple carboxylate conformations associated with each carbene conformation differ in energy by less than 1 kcal/mol. Conformation **21** has the lowest energy with **22** 3 kcal/mol higher in energy and **23** 14 kcal/mol higher still. A conformation in which the carbene is rotated 180° from its positioning in **22** was not found to be a conformational minimum. The main contributors to the difference in energy between **21** and **22** are van der Waals and dipolar forces. In **23**, there is significant angle bending, presumably to reduce van der Waals interactions.

Similar calculations were performed on $Rh_2(4R\text{-BNOX})_2(acam)_2{=}CHCOOMe$ to provide a comparison with the MEPY conformations **21–23**. The bis(acetamide) was employed with the expectation that the two benzyl groups on the opposite rhodium face would contribute little or no steric effect. Computations were performed as previously described. Three structures, similar in geometry to **21–23**, were identified as minima for this dirhodium(II) carbomethoxycarbene, **24–26** (Chart II), but their relative energies were considerably less than those of **21–23**. The "bisecting" conformation **24** has the same energy as the "parallel" conformation **25**, and conformation **26** is only 7 kcal/mol higher in energy. These lower energy differences stem from the ability of the benzyl group to rotate away from the active site of the catalyst and from the lack of a large dipole associated with the benzyl group.

Discussion

The effectiveness of dirhodium(II) catalysts that possess chiral oxazolidinone or pyrrolidone ligands for highly enantioselective metal–carbene transformations is demonstrated by the enantiomeric excesses that characterize their products (e.g, eqs 5–11, Table V). In this regard, $Rh_2(5S\text{-MEPY})_4$ and its enantiomer, $Rh_2(5R\text{-MEPY})_4$, are clearly superior to $Rh_2(4R\text{-BNOX})_4$ and its enantiomer, $Rh_2(4S\text{-BNOX})_4$ (or $Rh_2(4S\text{-IPOX})_4$). In addition, as suggested by results for intramolecular cyclopropanation of 3-methyl-2-buten-1-yl diazoacetate (eq 12), catalysis by $Rh_2(5R\text{-MEPY})_4$ is not subject to carbocation-derived competing processes.

Chart I

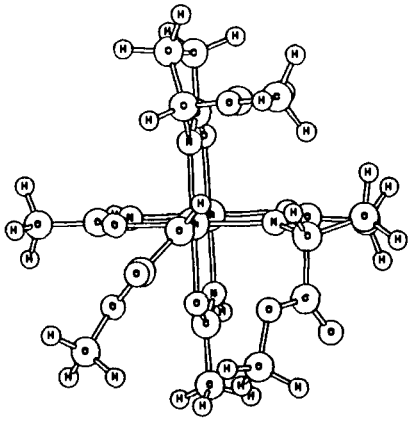

21

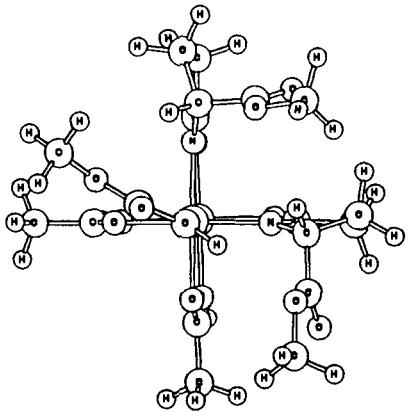

22

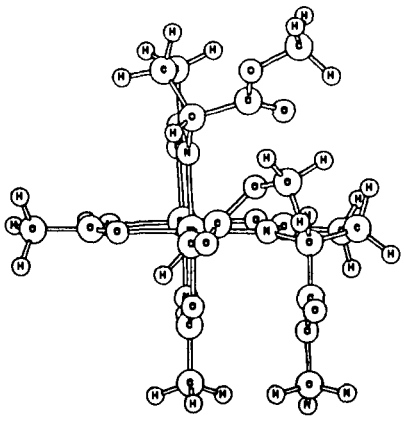

23

Chart II

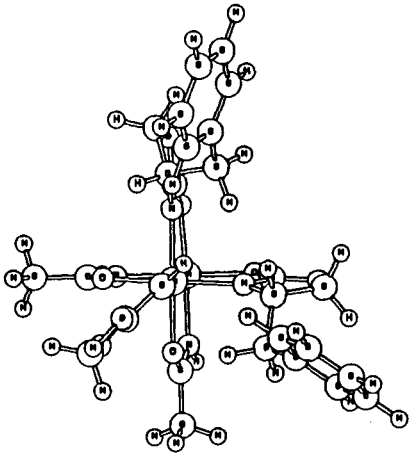

24

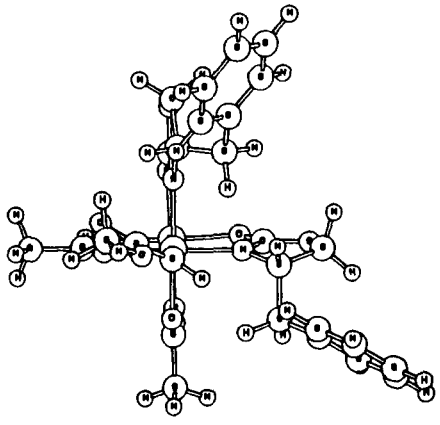

25

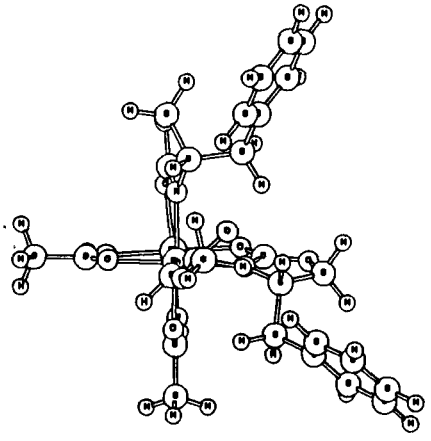

26

Scheme II

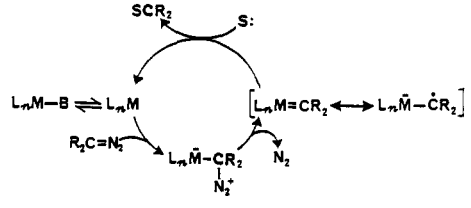

The X-ray structures of $Rh_2(5R\text{-MEPY})_4$ and $Rh_2(4S\text{-BNOX})_4$ demonstrate that the four chiral amide ligands are arranged with two nitrogens and two oxygens in a cis configuration. The ring attachments that give rise to stereodifferentiation in metal–carbene transformations, COOMe in the case of $Rh_2(5R\text{-MEPY})_4$ and CH_2Ph for $Rh_2(4S\text{-BNOX})_4$, describe a clockwise rotation around the carbene-bound rhodium face (see Figures 1 and 2 and **21–26**).

Since $Rh_2(5R\text{-MEPY})_4$ and $Rh_2(4S\text{-BNOX})_4$ can be recovered intact from catalytic reactions with diazo compounds and recent studies with polyethylene-bound dirhodium(II) 2-oxopyrrolidine-5(*S*)-carboxylate have demonstrated reuse of the same catalyst up to seven times without significant loss in enantioselectivity,[34] we view the mechanism for metal–carbene formation as occurring *without* cleavage of either Rh–N or Rh–O bonds but, instead, taking place by electrophilic addition of the coordinatively unsaturated dirhodium(II) catalyst onto the diazo compound.[25a,b,35] The equilibrium constant for acetonitrile association (Table IV) is a measure of the electrophilic character of these catalysts. Loss of dinitrogen produces the metal–carbene that, because of its integral electrophilic reactivity, is also depicted as a metal-stabilized carbocation (Scheme II).[5,15b,25]

Molecular mechanics calculations predict two minimum energy conformations, **27A** and **27B** in a simplified and generalized depiction of **21** and **22** or **24** and **25** (A = ring attachement), for MeOOCCH bound to $Rh_2(5R\text{-MEPY})_4$ and to $Rh_2(4S\text{-BNOX})_4$.

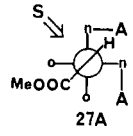

27A

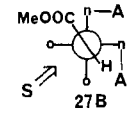

27B

In **27A**, access by a reactive substrate (S) to the top side of the carbene is less restrictive than is access to the bottom side where interference from the ligand attachment A inhibits approach. In **27B**, access to the bottom side is favored. The difference in the total energies for the limiting conformers of the carbomethoxycarbene-bound $Rh_2(5R\text{-MEPY})_4$ is 3 kcal/mol favoring **27A**, whereas that for the limiting conformers of the carbomethoxycarbene-bound $Rh_2(4S\text{-BNOX})_4$ is negligible. These calculations suggest that a higher level of enantiocontrol should be achieved

(34) Doyle, M. P.; Eismont, M. Y.; Bergbreiter, D. E.; Gray, H. N. *J. Org. Chem.* **1992**, *57*, 6103.

(35) Maxwell, J. L.; Brown, K. C.; Bartley, D. W.; Kodadek, T. *Science* **1992**, *256*, 1544.

Chart III

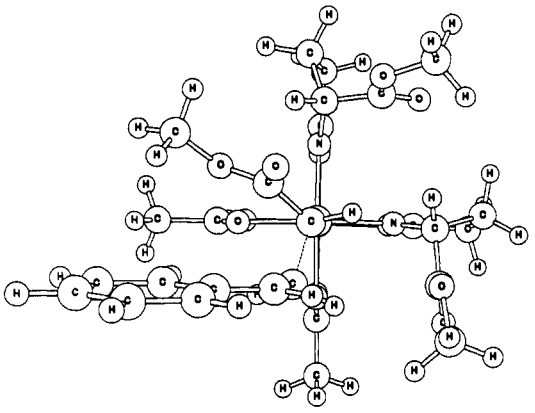

28

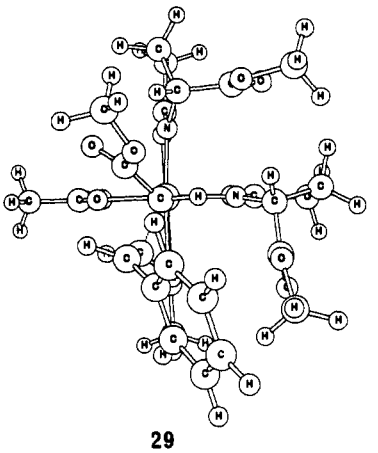

29

Scheme III

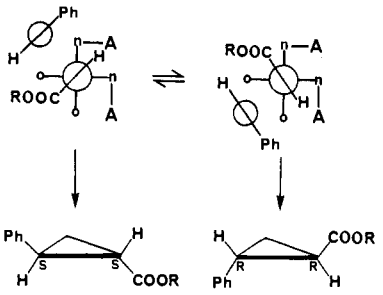

with the use of $Rh_2(5R\text{-MEPY})_4$, but the absolute configurations of the products obtained in the metal–carbene transformations are opposite to those predicted by preferential reactions through the limiting conformer **27A**. For example, in intermolecular cyclopropanation reactions, the positioning of styrene to form *trans*-2-phenylcyclopropanecarboxylate shows that alignment according to **27A** results in the (1*S*,2*S*)-configuration whereas alignment according to **27B** provides the observed (1*R*,2*R*)-configuration (Scheme III).

Conformer stabilities do not always correctly predict the favored product configuration. If the rates for product formation from two minimum energy conformers are significantly different, the lower energy conformer could be the one that results in the formation of the wrong enantiomer.[36] This is the case with the $Rh_2(MEPY)_4$ catalysts. Differences in conformational energies do not reflect enantiomer or diastereoisomer preference.

Molecular mechanics calculations of the rhodium–carbene weakly bonded to styrene, that were optimized from the geometry generalized in **27A** and **27B** and depicted specifically in Scheme III for formation of *trans*-2-phenylcyclopropane-1-carboxylate enantiomers, were performed in order to obtain conformational minima whose energy differences would reflect those in the transition state for cyclopropanation. Among all possible conformations, those leading to the observed product preference, (1*R*,2*S*)-*cis*- and (1*R*,2*R*)-*trans*-2-phenylcyclopropanecarboxylates, were the lowest in energy. For **20** to which is attached carbomethoxycarbene, the minimum energy structures for interaction with styrene are depicted in **28** and **29**. Thus, although **21** is the conformational energy minimum, **28** and **29** (which are derived from **22**) account for predominant product formation (Chart III).

Catalytic metal–carbene reactions of rhodium are believed to have an early transition state in transformations such as cyclopropanation.[37] The use of steric effects to control the approach of the reacting substrate onto the carbene center has been a principal focus of ligand design,[10-13,38,39] and with copper(I) semicorrins[11] and bis(oxazolines),[12,13] this approach has been highly successful for intermolecular cyclopropanation reactions. However, in catalytic asymmetric reactions other than those of metal–carbenes, the use of catalysts whose ligands possess functional groups that provide secondary attractive interactions is also a highly successful approach to high enantiocontrol in selected cases.[40]

Molecular mechanics calculations of the total energies of **27A** and **27B** lead to the inference that dipolar effects between the carboxylate group of the carbene and the ester attachment of the ligands in $Rh_2(5R\text{-MEPY})_4$ are primarily responsible for their large difference. With $Rh_2(4S\text{-BNOX})_4$, small electrostatic and steric interactions are offset by angle strain, whereas with $Rh_2(5R\text{-MEPY})_4$ these energies are much greater (1.9 kcal/mol) than angle strain. However, dipolar influences alone cannot explain the absence of butenolide **15** in $Rh_2(MEPY)_4$-catalyzed intramolecular cyclopropanation of 3-methyl-2-buten-1-yl diazoacetate (eq 12). With both $Rh_2(BNOX)_4$ and $Rh_2(4S\text{-IPOX})_4$, butenolide formation is significant, and its formation can be explained by the mechanism outlined in Scheme I.[41]

The absence of butenolide **15** in $Rh_2(MEPY)_4$-catalyzed reactions is consistent with ligand carbonyl group stabilization of the intermediate metal–carbene/metal-bound carbocation. The minimum distance between the ligand carbonyl oxygen and the carbene carbon is 3.1 Å in **27A** and **27B**. Interaction of the ligand carbonyl oxygen with the carbene can be viewed as stabilizing the transition state for electrophilic addition (thereby inhibiting butenolide formation), and this interaction would be expected to further orient the carbene for a greater degree of enantiocontrol.[5] However, analysis of the molecular orbitals from extended Hückel calculations did not show any interaction between the carbonyl oxygen p orbitals and the p orbital of the carbene, and thus, we are unable to confirm this interaction at the extended Hückel level of calculation. Well-known shortcomings of the extended Hückel method[42] do not permit structural optimization that would lead to more definitive evidence as to the existence of carbonyl stabilization of the metal–carbene. However, the

(36) Ashby, M. T.; Halpern, J. *J. Am. Chem. Soc.* **1991**, *113*, 589.
(37) Brown, K. C.; Kodadek, T. *J. Am. Chem. Soc.* **1992**, *114*, 8336.
(38) (a) O'Malley, S.; Kodadek, T. *Organometallics* **1992**, *11*, 2299. (b) Maxwell, J. L.; O'Malley, S.; Brown, K. C.; Kodadek, T. *Organometallics* **1992**, *11*, 645.
(39) Tokor, C. J.; Kettler, P. B.; Tolman, W. B. *Organometallics* **1992**, *11*, 2737.
(40) Sawamura, M.; Ito, Y. *Chem. Rev.* **1992**, *92*, 857.
(41) That this difference in butenolide formation is not due to the difference in the heterocyclic ligand, pyrrolidone versus oxazolidinone, was confirmed with the use of dirhodium(II) tetrakis(methyl 2-oxooxazolidine-4(*S*)-carboxylate)[22] which, like $Rh_2(MEPY)_4$ catalysts, did not produce butenolide **15**.
(42) Lowe, J. P. *Quantum Chemistry*; Academic Press: New York, 1978; p 301.

present data suggest that either dipolar effects or carbonyl oxygen stabilization could be responsible for the effectiveness of $Rh_2(MEPY)_4$ catalysts for highly enantioselective metal–carbene transformations.

Experimental Section

General Methods. ^1H NMR spectra were obtained from a 300-MHz spectrometer, and ^{13}C NMR spectra were recorded at 75 MHz. Mass spectra were obtained from a quadrupole instrument at an ionizing voltage of 70 eV. Infrared spectra were recorded on a FT instrument having a resolution of ±1 cm^{-1}. Microanalyses were performed at Texas Analytical Laboratories, Inc. Dirhodium(II) tetraacetate was obtained commercially or prepared from rhodium(III) chloride hydrate.[43] Oxazolidinones **2** and **3** were obtained from Aldrich Chemical Co. and used without further purification. Both (+)-2-pyrrolidone-5(*R*)-carboxylic acid and (–)-2-pyrrolidone-5(*S*)-carboxylic acid were recrystallized from ethanol prior to use: $[\alpha]^{22}_D = +10°$ or $-10°$, respectively (H_2O, $c = 0.97$). *d*-(+)-Menthyl diazoacetate and *l*-(–)-menthyl diazoacetate[44] were prepared from their corresponding diazoacetoacetate esters[18b] by deacylation in aqueous acetonitrile using 3.0 equiv of lithium hydroxide. Chlorobenzene, acetonitrile, and dichloromethane were distilled from calcium hydride prior to use. 1,2-Dichloroethane was distilled from phosphorus pentoxide.

Methyl 2-Oxo-pyrrolidine-5(*R*)-carboxylate (4R). To a 500-mL, one-neck, round-bottom flask was added (+)-2-pyrrolidone-5(*R*)-carboxylic acid (6.60 g, 51.1 mmol) and 200 mL of methanol. A catalytic amount of thionyl chloride (0.5 mL) was added to the rapidly stirred solution, the reaction flask was capped with a septum, and the resulting solution was stirred at room temperature for 24 h. Saturated aqueous Na_2CO_3 was added to reach a solution pH of 7, and methanol was removed under reduced pressure. The residue was dissolved in 50 mL of CH_2Cl_2 and washed with brine, the brine was then extracted twice with CH_2Cl_2, and the combined extract was washed with saturated aqueous Na_2CO_3 solution, dried over anhydrous $MgSO_4$, filtered, and concentrated under reduced pressure. Distillation afforded 6.22 g (43.4 mmol, 85% yield) of colorless product, bp 90 °C at 0.3 Torr, $[\alpha]^{22}_D = -9.7°$ (EtOH, $c = 1.10$) (lit.[45] $[\alpha]^{20}_D = -8.7°$ (EtOH, $c = 1.13$)). The same procedure was used for the preparation of the (*S*)-enantiomer.

Dirhodium(II) Tetrakis(methyl 2-oxopyrrolidine-5(*R*)-carboxylate) (Rh_2(5*R*-MEPY)$_4$). Rhodium(II) acetate (200 mg, 0.452 mmol), methyl 2-oxopyrrolidine-5(*R*)-carboxylate (1.02 g, 7.13 mmol), and 20 mL of anhydrous chlorobenzene were combined in a 50-mL, one-neck, round-bottom flask fitted with a Soxhlet extraction apparatus into which was placed a thimble containing 5 g of an oven-dried mixture of 2 parts Na_2CO_3 and one part sand. The resulting blue solution was heated at reflux under nitrogen for 16 h, after which the solvent was removed under reduced pressure to yield a blue glasslike solid. This solid was dissolved in a minimal volume of methanol and purified by chromatography on a column containing 10 g of J. T. Baker Bondapak-CN capped silica in methanol. Excess ligand eluted as a yellow-brown band and was collected in the first 100 mL of eluent. Subsequent elution with 1.0 vol % acetonitrile in methanol caused an instantaneous color change in the blue band across the top of the column to red and rapid elution. The entire red band was collected as one fraction, and the solvent was removed under reduced pressure to yield 250 mg of a blue glasslike solid that was 95% pure by HPLC analysis on a μ-Bondapak-CN column (eluent: 2% acetonitrile in methanol). This solid was then dissolved in 1.0 mL of acetonitrile per 100 mg of solid, and an equivalent amount of isopropyl alcohol was added. Bright red crystals formed overnight, and they were isolated by filtration and washed with isopropyl alcohol to yield 210 mg (0.23 mmol, 51% yield) of Rh_2(5*R*-MEPY)$_4$(CH_3CN)$_2$(*i*-PrOH). ^1H NMR ($CDCl_3$, 300 MHz): δ 4.32 (dd, $J = 8.8$, 3.0 Hz, 2H), 4.08–3.96 (m, 1H), 3.95 (dd, $J = 8.6$, 2.1 Hz, 2H), 3.70 (s, 6H), 3.68 (s, 6H), 2.70–2.55 (m, 4H), 2.26 (s, 6H), 1.8–2.4 (m, 12H), 1.35 (d, $J = 4.4$ Hz, 1H), 1.21 (d, $J = 6.1$ Hz, 6H). ^{13}C NMR ($CDCl_3$, 75 MHz): δ 188.6, 188.3, 175.5, 175.2, 115.4, 66.8, 66.7, 62.2, 51.9, 51.7, 31.6, 31.4, 26.0, 25.4, 25.2, 2.8. $[\alpha]^{23}_D = +259.5°$ (CH_3CN, $c = 0.098$). Anal. Calcd for $C_{31}H_{46}N_6O_{13}Rh_2$: C, 40.63; H, 5.06; N, 9.17. Found: C, 40.37; H, 5.11; N, 9.12. Dirhodium(II) tetrakis(methyl 2-oxopyrrolidine-5(*S*)-carboxylate) was prepared from methyl 2-pyrrolidone-5(*S*)-carboxylate and $Rh_2(OAc)_4$ by the same procedure and was characterized in the same manner. Although the $Rh_2(MEPY)_4$ product obtained after chromatography constitutes a nearly 70% yield and provides identical selectivities in metal–carbene reactions, the crystalline form is preferred because, as the acetonitrile complex, this catalyst form is stable indefinitely.

Dirhodium(II) Tetrakis(4(*S*)-benzyl-2-oxazolidinone) (Rh_2(4*S*-BNOX)$_4$). A mixture of rhodium(II) acetate (220 mg, 0.498 mmol) and (*S*)-4-benzyl-2-oxazolidinone (0.886 g, 5.00 mmol) in 20 mL of anhydrous chlorobenzene was refluxed under nitrogen in a 100-mL, one-neck, round-bottom flask fitted with a Soxhlet extraction apparatus. The thimble was charged with 5 g of an oven-dried mixture of two parts Na_2CO_3 and one part sand. After 24 h, the resulting blue solution was cooled to room temperature and the solvent was removed in vacuo. The resulting solid was dissolved in a minimum of methanol and purified by chromatography on a column containing 10 g of J. T. Baker Bondapak-CN capped silica. The ligand eluted as a colorless band in the first 100 mL, and the catalyst eluted as a broad red band upon addition of 1% acetonitrile in methanol. The entire red band was collected as one fraction and the solvent removed to yield 200 mg of a material 99% pure by HPLC analysis on a μ-Bondapak-CN column (eluent: 2% acetonitrile in methanol). This solid was dissolved in acetonitrile (1 mL per 100 mg) to produce a deep red solution which yielded 174 mg (0.18 mmol, 35% yield) of deep red crystals of Rh_2(4*S*-BNOX)$_4$(CH_3CN)$_2$ upon cooling to 10 °C overnight. ^1H NMR ($CDCl_3$, 300 MHz): δ 7.37–7.17 (m, 20H), 4.22–3.98 (m, 8H), 3.80–3.73 (m, 2H), 3.34 (dd, $J = 14.0$, 3.0 Hz, 2H), 3.14 (dd, $J = 13.5$, 3.0 Hz, 2H), 2.43 (dd, $J = 10.1$, 13.7 Hz, 2H), 2.31 (dd, $J = 10.9$, 13.8 Hz, 2H), 2.27 (s, CH_3CN). ^{13}C NMR ($CDCl_3$, 75 MHz): δ 167.3, 138.5, 137.9, 129.0, 128.8, 128.6, 126.7, 126.6, 126.4, 116.0, 69.5, 69.2, 63.3, 61.6, 41.4, 41.1, 2.7. $[\alpha]^{23}_D = +147° \pm 3°$ (CH_3CN, $c = 0.132$). Anal. Calcd for $C_{40}H_{40}N_4O_8Rh_2$: C, 52.76; H, 4.42; N, 6.15. Found: C, 52.35; H, 4.50; N, 6.06. Dirhodium(II) tetrakis(4(*R*)-benzyl-2-oxazolidinone) was prepared from (*R*)-4-benzyl-2-oxazolidinone and $Rh_2(OAc)_4$ by the same procedure and was characterized in the same manner. The product after chromatography, prior to recrystallization, was obtained in greater than 70% yield.

Dirhodium(II) Tetrakis(4(*S*)-isopropyl-2-oxazolidinone) (Rh_2(4*S*-IPOX)$_4$). A mixture of rhodium(II) acetate (150 mg, 0.34 mmol) and (*S*)-4-isopropyl-2-oxazolidinone (438 mg, mmol) in 30 mL of anhydrous chlorobenzene was treated as previously described for Rh_2(4*S*-BNOX)$_4$. The resulting solid was purified by chromatography on 10 g of J. T. Baker Bondapak-CN capped silica in methanol. Excess ligand eluted with methanol and was contained in the first 100 mL of solvent. Subsequent elution with 1.0 vol % acetonitrile in methanol caused an instantaneous color change to red and rapid elution. The entire red band was collected as one fraction, and the solvent was removed under reduced pressure to give 0.24 g of a blue glass constituting a 98% yield. ^1H NMR ($CDCl_3$, 300 MHz): δ 4.17–4.04 (m, 8H), 3.64–3.58 (m, 2H), 3.49–3.45 (m, 2H), 2.29–2.21 (m, 2H), 2.19–2.05 (m, 2H), 0.89 (d, $J = 7.0$ Hz, 6H), 0.84 (d, $J = 7.0$ Hz, 6H), 0.72 (d, $J = 7.0$ Hz, 6H), 0.68 (d, $J = 7.0$ Hz, 6H). ^{13}C NMR ($CDCl_3$, 75 MHz): δ 167.0, 166.8, 66.0, 65.0, 64.6, 30.4, 29.7, 19.1, 18.7, 14.2, 13.7. $[\alpha]^{23}_D = +216.9°$ (CH_3CN, $c = 0.201$). Anal. Calcd for $C_{24}H_{40}O_8N_4Rh_2$: C, 40.12; H, 5.61; N, 7.80. Found: C, 40.06; H, 5.70; N, 7.74.

X-ray Determinations. Details of the crystal data, data collection, and data refinement are listed in Table I. Data reduction and decay corrections were performed using the SHELXTL-PLUS software package.[46] The structures were solved by direct methods and refined by full-matrix least squares.[46] Non-hydrogen atoms were refined with anisotropic thermal parameters; the idealized positions of the hydrogen atoms were calculated using distances of 0.96 Å for C–H and 0.90 Å for N–H and assigning isotropic thermal parameters = $1.2U_{eq}$ of the bonded non-hydrogen atom. Positions and thermal parameters were not refined. The function, $\sum w(|F_o| - |F_c|)^2$, was minimized, where $w = 1/(\sigma(F_o))^2$ and $\sigma(F_o) = 0.5kI^{-1/2}[(\sigma(I))^2 + (0.021)^2]^{1/2}$. The intensity I is given by $(I_{peak} - I_{background})$(scan rate); 0.02 is a factor to downweight intense reflections and to account for instrument instability, and k is the correction due to Lp effects, absorption, and decay. $\sigma(I)$ was estimated from counting statistics; $\sigma(I) = I_{peak} + I_{background})^{1/2}$(scan rate). The absolute configuration was determined by Rogers' η refinement procedure[47] using the anomalous scattering of the Rh atoms. Neutral atom scattering factors for the non-H atoms were taken from Cromer and Mann,[48] with the anomalous-dispersion corrections

(43) Rampel, G. A.; Legzdins, P.; Smith, H.; Wilkinson, G. *Inorg. Synth.* **1972**, *13*, 90.
(44) Fritschi, H.; Leutenegger, U.; Pfaltz, A. *Helv. Chim. Acta* **1988**, *71*, 1553.
(45) Ackerman, Y.; Matthes, M.; Tamm, C. *Helv. Chim. Acta* **1990**, *73*, 122.
(46) Sheldrick, G. M. SHELXTL-*PLUS*, Version 4.11; Siemens X-ray Analytical Instruments, Inc.: Madison, WI, 1991.
(47) Rogers, D. *Acta Crystallogr.* **1981**, *A37*, 734.
(48) Cromer, D. T.; Mann, J. B. *Acta Crystallogr.* **1968**, *A24*, 321.

taken from the work of Cromer and Liberman.[49] The scattering factors for the H atoms were obtained from Steward, Davidson, and Simpson.[50] Values used to calculate the linear absorption coefficient are from the *International Tables for X-ray Crystallography* (1974).[51] All figures were generated using SHELXTL-PLUS. Other computer programs used in this work are listed elsewhere.[52]

$(C_6H_8NO_3)_4Rh_2(CH_3CN)_2((CH_3)_2CHOH)$ (5). Large reddish crystals were grown by crystallization from an acetonitrile/2-propanol solution. A carboxylate group on one ligand is conformationally disordered. The pyrrolidine ring is in the envelope conformation with the carboxylate group bound to the flap atom. The disorder is such that in one orientation, the flap atom is above the plane of the remaining atoms of the pyrrolidinone ring, and in the second orientation, it is below this plane. One carboxylate group is rotated by approximately 180° with respect to the other about the C_{ring}–$C_{carboxylate}$ bond. The carbonyl oxygen of the major component is very close to the ester oxygen of the minor component; also, the methyl carbons are very close to each other. The atoms of the major conformer (55(1)%) are labeled C17′–C22′, whereas those of the minor conformer are labeled C17A–C22A. In addition, one solvate molecule of 2-propanol is severely disordered about two principal orientations. Peaks that were close to the carbonyl oxygens of the ligand were assumed to be oxygen atoms, and the peaks nearest to them were assumed to be the central carbons of the alcohol. The remaining carbons were assigned similarly. Because the subsequent refinement resulted in highly distorted geometries, idealized geometries for the alcohols were calculated and subsequently refined as rigid groups. The groups site occupancies refined to very nearly 50% and were fixed at 0.5 for the remainder of the refinement. No H atoms were calculated for any atoms of the solvent.

$(C_{10}H_{10}NO_2)_4Rh_2(CH_3CN)_2(CH_3CN)$ (6). A prismatic red crystal was recrystallized from an acetonitrile solution. No disorder was present.

Equilibrium Constants for Association with Acetonitrile. Crystalline $Rh_2(5R\text{-MEPY})_4(CH_3CN)_2(i\text{-PrOH})$ or $Rh_2(4S\text{-BNOX})_4(CH_3CN)_2(CH_3CN)$ was weighed (20–30 mg) into a 10-mL, round-bottom flask and dissolved in methanol. The methanol was evaporated under reduced pressure, and this procedure was repeated once with methanol and three times with dichloroethane to aid the removal of the axial acetonitrile ligands of the dirhodium(II) compounds. The solid residue was heated at 60 °C overnight in a vacuum oven (25 Torr) to produce final color changes from red to green with $Rh_2(4S\text{-BNOX})_4$ and to blue/green with $Rh_2(5R\text{-MEPY})_4$. While still warm, the flask was transferred to a glovebox, and after cooling to room temperature, the solid dirhodium(II) compound was dissolved in 5.00 ± 0.05 mL of dichloroethane. From this solution, 3.00 ± 0.05 mL was transferred to a dry cuvette that was sealed with a septum. Spectra were recorded from 400 to 700 nm on a diode array spectrophotometer with a cell temperature of 25.0 °C. Sequentially, 5.0 ± 0.1 μL of a stock solution of acetonitrile (0.765 M) in dichloroethane was added, the spectrum was recorded after thorough mixing, and the spectral data were then stored. After the addition of 10 aliquots of this stock solution, pure undiluted acetonitrile was added in 10 increments of 5.0 ± 0.1 μL and the resulting spectra were recorded following each addition. Measurements were performed in duplicate or triplicate.

Equilibrium constants for K_1 were determined from a plot of $1/\Delta A$ versus $1/[CH_3CN]$, which yielded a straight line ($r > 0.99$) with intercept/slope equal to K_1. For the determination of K_2, a similar equation was derived so that a plot of $1/\Delta A$ versus $[CH_3CN]$ yielded a straight line ($r > 0.99$) with slope/intercept equal to K_2. For K_1 determinations, absorbance values were taken at 610–640 nm; absorbance values for determination of K_2 were obtained at 480–490 nm. Using calculated equilibrium constants, we determined the percentages of each ligated dirhodium(II) species as a function of acetonitrile concentration. These results testify to the validity of K_1 determinations but suggest that K_2 values could be skewed somewhat due to as much as 11% unligated dirhodium(II) during the initial data accumulation for K_2.

Intermolecular Cyclopropanation of Styrene with *d*- and *l*-Menthyl Diazoacetate. To a light blue solution of styrene (10.0 mmol) and dirhodium(II) catalyst (0.005 mmol) in 5 mL of refluxing CH_2Cl_2 under nitrogen was added *d*- or *l*-methyl diazoacetate (0.50 mmol) in 5 mL of CH_2Cl_2 through a syringe pump at a rate of 0.7 mL/h. After addition was complete, the reaction mixture was filtered through a 1-cm silica plug to separate the catalyst and the plug was eluted with 30 mL of CH_2Cl_2. A standard, ethyl *trans*-2-phenylcyclopropanecarboxylate (0.156 mmol), was added, and the dichloromethane solution was evaporated under reduced pressure. The resulting mixture was analyzed by GC on a 30-m capillary methylsilicone column from which the order for elution of diastereomeric cyclopropane products was (1*R*,2*S*)-**7** and then (1*S*,2*R*)-**7** followed by (1*S*,2*S*)-**7** and then (1*R*,2*R*)-**7** or (1*S*,2*R*)-**8** and then (1*R*,2*S*)-**8** followed by (1*R*,2*R*)-**8** and then (1*S*,2*S*)-**8** (base-line separation). Using a previously determined response factor for the standard of 1.63, we determined percentage yields of the menthyl 2-phenylcyclopropanecarboxylates (32–74%).[20] The chromatographic and spectral characteristics of the cyclopropane products **7** and **8** have been previously reported.[44]

Intermolecular Cyclopropenation of 1-Hexyne with Ethyl Diazoacetate. To a light blue solution of 1-hexyne (15.0 mmol) and dirhodium(II) catalyst (0.01 mmol) in 10 mL of anhydrous CH_2Cl_2 at room temperature under nitrogen was added ethyl diazoacetate (1.6 mmol) in 5 mL of CH_2Cl_2 through a syringe pump at a rate of 1.0 mL/h. After addition was complete, the reaction mixture was filtered through a 1-cm silica plug to separate the catalyst and the plug was eluted with 70 mL of CH_2Cl_2. The dichloromethane solution was then evaporated under reduced pressure, and the resulting cyclopropene-3-carboxylate ester was purified by column chromatography on silica gel with hexane–ethyl acetate (10:1) as the eluent. **Ethyl 1-*n*-butylcyclopropene-3-carboxylate (9)** was obtained in 60% isolated yield as the sole product of the reaction with $Rh_2(5S\text{-MEPY})_4$. ^1H NMR ($CDCl_3$, 300 MHz): δ 6.34 (q, J = 1.4 Hz, 1H), 4.14 (dq, J = 7.1, 3.1 Hz, 2H), 2.51 (dt, J = 7.1, 1.4 Hz, 2H), 2.14 (d, J = 1.5 Hz, 1H), 1.58 (quintet, J = 7.1 Hz, 2H), 1.40 (sextet, J = 7.0 Hz, 2H), 1.27 (t, J = 7.1 Hz, 3H), 0.93 (t, J = 7.2 Hz, 3H). IR (neat): 3142, 1804 (C=C), 1732 (C=O) cm^{-1}. Mass spectrum, m/e (rel abundance): 168 (1.2, M – 16), 139 (5), 125 (10), 97 (80), 95 (100), 67 (30), 55 (40), 53 (61). $[\alpha]^{23}_D$ = +3.58° ($CHCl_3$, c = 0.99) for 56.7% ee. Product decomposed upon attempted purification to obtain an analytical sample. Enantiomeric excesses were determined with the use of chiral NMR shift reagent Eu(tfc)$_3$ on the vinylic proton and by gas chromatographic separation on a Chiraldex γ-cyclodextrin trifluoroacetate column with correspondence to within ±2%.

Intramolecular Cyclopropanation of 3-Methyl-2-buten-1-yl Diazoacetate. To a light blue solution of the dirhodium(II) catalyst (0.015 mmol) in 30 mL of refluxing anhydrous CH_2Cl_2 under nitrogen was added 3-methyl-2-buten-1-yl diazoacetate (1.5 mmol) in 5 mL of CH_2Cl_2 through a syringe pump at a rate of 0.40 mL/h. During the course of the addition, the reaction solution turned from blue to green and back to blue after the addition was complete. After addition was complete, the reaction solution was filtered through a 1-cm silica plug and the plug was eluted with an additional 30 mL of CH_2Cl_2. The resulting dichloromethane solution was evaporated under reduced pressure, and the residue was purified by column chromatography on silica gel with hexane–ethyl acetate (5:1 graduated to 3:1) as the eluent. The major fraction was further purified by bulb-to-bulb distillation: bp 120 °C (15 Torr); lit.[53] bp 105 °C (10 Torr). **(1*S*,5*R*)-(+)-6,6-Dimethyl-3-oxabicyclo[3.1.0]hexan-2-one (10)** was obtained in 82% isolated yield as the sole product of the reaction with $Rh_2(5S\text{-MEPY})_4$. $[\alpha]^{23}_D$ = +88.5° ($CHCl_3$, c = 1.01); 98.4% ee, based on optically pure **9**, $[\alpha]^{25}_D$ = +89.9° ($CHCl_3$, c = 1.4).[54] Separation of the enantiomers occurred on a 30-m Chiraldex γ-cyclodextrin trifluoroacetate capillary column from which the % ee was calculated to be 98.6. ^1H NMR ($CDCl_3$, 300 MHz): δ 4.36 (dd, J = 9.8, 5.5 Hz, 1H), 4.15 (d, J = 9.8 Hz, 1H), 2.04 (dd, J = 6.2, 5.5 Hz, 1H), 1.95 (d, J = 6.2 Hz, 1H), 1.18 (s, 3H), 1.17 (s, 3H).

Reactions catalyzed by $Rh_2(4R\text{-BNOX})_4$, $Rh_2(4S\text{-BNOX})_4$, and $Rh_2(4S\text{-IPOX})_4$ produced butenolide **15** in addition to the product from intramolecular cyclopropanation. ^1H NMR ($CDCl_3$, 300 MHz): δ 5.81 (q, J = 1.6 Hz, 1H), 4.79 (d, J = 1.8 Hz, 2H), 2.69 (d of heptets, J = 7.2, 1.6 Hz, 1H), 1.22 (d, J = 7.2 Hz, 6H). Mass spectrum, m/e (rel abundance): 127 (3, M + 1), 126 (M, 16), 111 (33), 97 (82), 84 (56), 82 (35), 81 (68), 69 (39), 67 (81), 55 (54), 53 (100). The yield of this product was determined by GC and NMR analyses prior to purification by column chromatography.

Intramolecular Cyclopropanation of 3-Methyl-3-buten-1-yl Diazoacetate. Catalytic cyclopropanation reactions were performed in the same manner as those for the synthesis of **10**, and **(1*S*,6*R*)-6-methyl-3-oxabicyclo[4.1.0]heptan-2-one (11)**[21] was isolated in 76% yield by bulb-to-bulb distillation, bp 55 °C at 0.05 Torr. ^1H NMR ($CDCl_3$, 300 MHz): δ 4.24 (ddd, J = 12.1, 5.8, 1.5 Hz, 1H), 4.05 (dt, J = 12.5, 3.7

(49) Cromer, D. T.; Liberman, D. *J. Chem. Phys.* **1970**, *53*, 1891.
(50) Stewart, R. F.; Davidson, E. R.; Simpson, W. T. *J. Phys. Chem.* **1965**, *42*, 3175.
(51) International Tables for X-ray Crystallography; Kynoch Press: Birmingham, 1974; Vol. IV, p 55.
(52) Gadol, S. M.; Davis, R. E. *Organometallics* **1982**, *1*, 1607.
(53) Sabbioni, G.; Jones, B. *J. Org. Chem.* **1987**, *52*, 4565.
(54) Mukaiyama, T.; Yamashita, H.; Asami, M. *Chem. Lett.* **1983**, 385.

Hz, 1H), 2.05 (dt, J = 13.5, 5.8 Hz, 1H), 1.92 (dd, J = 14.0, 3.7 Hz, 1H), 1.68 (dd, J = 9.4, 4.5 Hz, 1H), 1.61 (dd, J = 10.1, 4.5 Hz, 1H), 1.29 (s, 3H), 0.99 (dd, J = 9.4, 5.5 Hz, 1H). ^{13}C NMR ($CDCl_3$, 75 MHz): δ 171.6, 64.6, 27.1, 23.9, 23.4, 21.8, 15.4. IR (thin film): 1712 cm^{-1} (C=O). Enantiomeric excesses were determined by GC separation on a 30-m Chiraldex γ-cyclodextrin trifluoroacetate capillary column.

Intramolecular Carbon–Hydrogen Insertion of 2-Methoxy-1-ethyl Diazoacetate. To a light blue solution of the dirhodium(II) catalyst (0.020 mmol) in 10 mL of refluxing anhydrous CH_2Cl_2 under nitrogen was added 2-methoxy-1-ethyl diazoacetate (2.0 mmol) in 5 mL of CH_2Cl_2 through a syringe pump at a rate of 0.5 mL/h. After addition was complete, the reaction solution was filtered through a 1-cm plug of neutral alumina to separate the catalyst and the plug was further eluted with 20 mL of chloroform. The combined organic solution was evaporated under reduced pressure, and the residue was purified by bulb-to-bulb distillation to afford a colorless liquid, bp 85 °C (0.3 Torr), identified as **4-methoxydihydro-2(3*H*)-furanone (12).** ^{1}H NMR ($CDCl_3$, 300 MHz): δ 4.36 (dd, J = 3.4, 1.7 Hz, 2H), 4.20–4.15 (m, 1H), 3.34 (d, J = 1.2 Hz, 3H), 2.68 (ddd, J = 18.0, 6.0, 1.5 Hz, 1H), 2.57 (dt, J = 18.0, 2.2 Hz, 1H). Mass spectrum, m/e (rel abundance): 117 (0.2, M + 1), 116 (3.3, M), 88 (8, M – CO), 85 (12), 59 (6), 58 (100), 57 (3), 55 (4). IR (thin film): 1778 cm^{-1} (C=O). Anal. Calcd for $C_5H_8O_3$: C, 51.72; H, 6.90. Found: C, 51.58; H, 6.78. With $Rh_2(5S\text{-MEPY})_4$, $[\alpha]^{23}_D = -58.6°$ (EtOH, c = 2.22) for 91% ee. Enantiomeric excesses were determined by GC separation on a 30-m Chiraldex γ-cyclodextrin trifluoroacetate capillary column. Further purification of the lactone was accomplished by column chromatography on silica gel using ether as the eluent.

Intramolecular Carbon–Hydrogen Insertion of *N*-*n*-Butyl-*N*-*tert*-butyldiazoacetamide. To a light blue solution of the dirhodium(II) catalyst (0.005 mmol) in 15 mL of refluxing anhydrous CH_2Cl_2 under nitrogen was added *N*-*n*-butyl-*N*-*tert*-butyldiazoacetamide (0.50 mmol) in 5 mL of CH_2Cl_2 through a syringe pump at a rate of 0.4 mL/h. After addition was complete, the blue reaction solution was filtered through a 1-cm silica plug and the plug was eluted with an additional 20 mL of CH_2Cl_2. The resulting dichloromethane solution was evaporated under reduced pressure to produce a residue which consisted of two products whose relative yields were determined on a methylsilicone column and whose % ee's were obtained by chromatographic separation on a Chiraldex γ-cyclodextrin trifluoroacetate column. ***N*-*tert*-Butyl-4-ethyl-2-pyrrolidone (13).** ^{1}H NMR ($CDCl_3$, 300 MHz): δ 3.57 (dd, J = 9.5, 7.8 Hz, 1H), 3.04 (dd, J = 9.5, 6.9 Hz, 1H), 2.47 (dd, J = 15.9, 7.8 Hz, 1H), 2.11 (heptet, J = 7.6 Hz, 1H), 2.02 (dd, J = 15.9, 7.9 Hz, 1H), 1.43 (quintet, J = 7.4 Hz, 2H), 1.38 (s, 9H), 0.91 (t, J = 7.4 Hz, 3H). ^{13}C NMR ($CDCl_3$, 300 MHz): δ 174.8, 53.7, 51.3, 39.4, 32.9, 27.6, 27.4, 11.6. Mass spectrum, m/e (rel abundance): 155 (10, M + 1), 154 (100, M), 126 (27), 114 (25), 97 (15), 69 (13), 58 (30), 57 (21), 56 (12), 55 (48). IR (thin film): 1686 cm^{-1} (C=O). Anal. Calcd for $C_{10}H_{19}NO$: C, 70.96; H, 11.31; N, 8.28. Found: C, 70.82; H, 11.36; N, 8.31. ***N*-*tert*-Butyl-4-*n*-propyl-2-azetidinone (14)** could not be completely separated from **12**, and its structure was inferred from spectroscopic data. ^{1}H NMR ($CDCl_3$, 300 MHz): δ 3.63–3.56 (m, 1H), 2.85 (dd, J = 14.3, 5.2 Hz, 1H), 2.36 (dd, J = 14.3, 2.3 Hz, 1H), 1.55–1.30 (m, 4H), 1.35 (s, 9H), 0.95 (t, J = 7.2 Hz, 3H). Mass spectrum, m/e (rel abundance): 155 (3, M + 1), 154 (31, M), 112 (36), 84 (60), 70 (46), 58 (15), 57 (100), 55 (38).

Calculations were performed using the Tektronix CAChe System, Version 3.0. Organometallic structures used in all calculations were obtained by minimization using the Molecular Mechanics packages provided. CAChe uses an augmented version of Allinger's MM2 force field[27] whereby force-field parameters are estimated for cases not explicitly addressed by MM2 (i.e., octahedrally disposed nuclei). In these calculations, rhodium was given a 2+ charge, each carboxamide ligand carried a negative charge, and the carbene carbon had a double bond to rhodium. The molecular orbital calculations were performed using the extended Hückel[55] methods provided. H_{ii}'s and orbital exponents used in the extended Hückel calculations are listed elsewhere.[23]

Acknowledgment. Support for this research by the National Science Foundation and the National Institutes of Health (GM 46503) to M.P.D. is gratefully acknowledged. S.H.S. and R.G. acknowledge the support of the Robert A. Welch Foundation. We wich to thank A. P. Kazala for her preliminary work with equilibrium measurements and for her preparation of dirhodium(II) catalysts.

Supplementary Material Available: Tables of positional and thermal parameters and bond lengths and angles (supplementary Tables 1–10), views of **5** and **6** showing the atom-labeling scheme and unit cell packing diagrams (supplementary Figures 1–4), tables of calculated coordinates for $Rh_2(5R\text{-MEPY})_4(CH_3CN)_2$, $Rh_2(4S\text{-BNOX})_4(CH_3CN)_2$, and **21–26** (supplementary tables 13–20), and tables of parameters for molecular mechanics calculations (supplementary Tables 20–23) (48 pages); tables of observed and calculated structure factor amplitudes (Supplementary Tables 11 and 12) (38 pages). Ordering information is given on any current masthead page.

(55) (a) Hoffmann, R. *J. Chem. Phys.* **1963**, *39*, 1397. (b) Hoffman, R.; Lipscomb, W. N. *J. Chem. Phys.* **1962**, *36*, 3179, 3489; **1962**, *37*, 2872.